

Process Monitoring of Tubular Microreactors using Particle Filter

Osamu Tonomura. Jun-ichi Kano.
Manabu Kano. Shinji Hasebe

*Department of Chemical Engineering, Kyoto University,
Kyoto 615-8510, Japan (e-mail: tonomura@cheme.kyoto-u.ac.jp).*

Abstract: Microreactors consist of tens to hundreds of micrometer-scale channels. The residence time of a fluid can be set exactly and backmixing can be minimized. Particularly, very short residence time can be achieved. In addition, it is possible to precisely control the reaction temperature due to large surface to volume ratio of channels. These features of microreactors make it possible to realize the production of specialty chemicals, which cannot be handled in conventional reactors. The most recognized problem in microreactors is channel blockage. The catalyst deterioration is also an inevitable problem for catalyst reactions in microreactors. To realize stable long-term operation of microreactors, it is necessary to detect such problems as early as possible. Since miniaturized sensors are expensive and their direct installation inside channels may disturb the flow, it is indispensable to develop a process monitoring system using a few indirect measurements. In this research, a state and parameter estimation system for tubular microreactors (TMRs) is developed to detect process faults. In the developed system, a process model is derived from the first-principle model of TMRs. Particle Filter (PF) or Extended Kalman Filter (EKF) or Ensemble Kalman Filter (EnKF) is designed to obtain the unknown parameters such as catalyst efficiency from a single wall temperature sensor. To achieve high estimation performance, the optimal sensor location is determined on the basis of the observability. The numerical examples illustrate that the blockage and the catalyst deterioration of TMRs can be detected more rapidly and accurately by using PF, as compared with EnKF and EKF.

Keywords: Microreactors, Process monitoring, State estimation, Parameter estimation, Particle filter

1. INTRODUCTION

The production of specialty chemicals such as cosmetics and medicines needs to be flexible toward market changes and be environmentally friendly. However, conventional reactors often generate a lot of by-products because of inadequate control of mixing and temperature. As an alternative, microreactors attract industrial attention and are suitable for the production of specialty chemicals (Miyake and Togashi, 2006). Microreactors (MRs) consist of tens to hundreds of micrometer-scale channels. Their main characteristics are rapid mixing and accurate temperature control (Miyake and Togashi, 2006). Therefore, microreactors can realize the production of specialty chemicals, which cannot be handled in conventional reactors, with a negligible amount of by-products. In addition, there is a difference between conventional reactors and microreactors in the ways of increasing the production capacity. Although the scale-up approach is well known in conventional reactors, it is time-consuming and has the possibility that the product quality is degenerated. On the other hand, numbering-up approach is adopted in the case of microreactors. Numbering-up approach involves the parallelization of microreactors and realizes smooth transition from laboratory scale to production scale without degeneration of the product quality.

To apply microreactors to real production and realize stable long-term operation, it is necessary to monitor process faults

such as blockage and catalyst deterioration, which are the critical problems in the operation of microreactors. The blockage and the catalyst deterioration are detected through the flow meters and the concentration analyzers installed in microchannels, respectively. However, the installation of such sensors disturbs the flow, and the existing miniaturized sensors are expensive. Therefore, it is desirable to estimate the inner operation condition of MRs from a limited number of indirect measurements. So far, there are few researches on fault detection and diagnosis of microreactors (Kano et al., 2007).

In this work, a physical model-based process monitoring system for tubular microreactors (TMRs) is developed to detect process faults. The monitoring performance depends on the accuracy of state and parameter estimation, which is done by various filters. Kalman filter is the optimal filter for linear systems subject to Gaussian distribution of the state. For nonlinear processes, extended Kalman filter (EKF) linearizes their nonlinear terms and applies Kalman filter. The estimated value of EKF tends to diverge when the system has strong nonlinearity. Whereas, ensemble Kalman filter (EnKF) does not linearize the nonlinear terms and has been used in forecasting (Yumimoto, 2009). Although the state distribution is not generally Gaussian for nonlinear processes, EKF and EnKF approximate the state distribution by Gaussian distribution. Particle filter (PF) does not linearize the nonlinear terms and does not assume a fixed shape of the state distribution. PF has been used in many

areas including signal and image processing and target recognition (Rawlings and Bakshi, 2006). However, only a few papers report applications of PF in the chemical industry. From these view points, in this work, PF is used to detect the blockage and the catalyst deterioration of TMRs. In addition, the monitoring performance is also influenced by the position of sensors. In this work, a single sensor is used to measure wall temperature. The problem of where to locate a temperature sensor along TMRs to estimate unknown parameters most accurately is investigated on the basis of the observability.

2. PARTICLE FILTER

Consider the following nonlinear state space model:

$$x_n = f(x_{n-1}) + w_{n-1} \tag{1}$$

$$y_n = h(x_n) + v_n \tag{2}$$

where x and y are the state and the measurement, respectively. f and h are the nonlinear functions of x . w and v represent system and measurement noise, respectively. n is the discrete time.

PF have attracted attention because of the recent improvement of computer performance. Unlike other nonlinear filters, PF does not assume a fixed shape of the probability densities of the states, but it approximates the probability densities via particles. The position and weight of particle present the value and probability density of state, respectively.

Figure 1 shows the schematic diagram of Monte Carlo Filter (MCF) which is a kind of PF. The basic algorithm is as follows:

- 1) Predicting the prior estimate $x_{n|n-1}$ at time n based on Eq. (1),
- 2) Evaluating each particle weight proportional to the likelihood (goodness of fit to the measurement y_n of the prior estimate $x_{n|n-1}$) of each particle,
- 3) Resampling the particles proportional to the particle weight so that the particles with very small weight are removed.

3. NUMERICAL EXAMPLE

In this section, PF is used in a numerical example and is compared with EKF in terms of the estimation performance.

3.1 Problem Setting

Consider the following nonlinear state space model (Kitagawa and Takemura, 2008):

$$x_n = 0.5x_{n-1} + \frac{25x_{n-1}}{1+x_{n-1}^2} + \cos\{1.2n\} + w_{n-1} \tag{3}$$

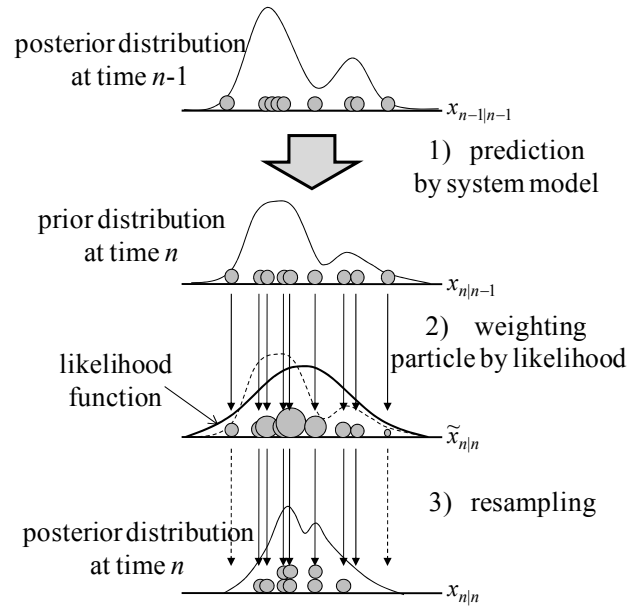


Fig. 1. Schematic diagram of MCF (Kitagawa and Takemura, 2008).

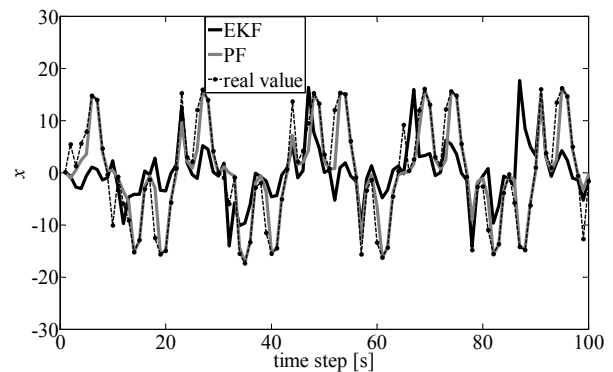


Fig. 2. Estimation results of EKF and PF.

Table 1. MSE and CPU time for state estimation.

	EKF	PF
MSE	109	51
CPU time	3.60E-05	2.50E-03

$$y_n = \frac{x_n^2}{20} + v_n \tag{4}$$

where w and v are zero-mean Gaussian white noise with variances 10 and 1, respectively. The initial state x_0 is 0.1 with variance 1.

This example is severely nonlinear both in Eq. (3) and Eq. (4). Equation (3) describes that the sign of the state sometimes changes. However, measurement, obtained from square of state through Eq. (4), does not have the sign information of state.

3.2 Results and Discussion

The average estimation results based on 100 simulations with different seeds of random numbers of system and measurement noise are shown in Fig. 2 and Table 1. Figure 2 shows the real value of the state and the estimation results of EKF and PF. In addition, Table 1 shows the Mean-Squares Error (MSE) and CPU time of each filter. The unit of CPU time is sec/time step. In PF, the number of particles is 100.

As shown in MSE of Table 1, the state estimation performance of PF is higher than that of EKF. In addition, the state estimation value of PF follows the sign change of real value at time step = 85-86 in Fig. 2, whereas the state estimation value of EKF changes in the direction opposite to the sign change of real value. The reason is as follows. In the state estimation, it is preferable that the state distribution has two peaks, positive and negative, because the only 1 step measurement does not have the sign information of the state. In EKF, the state distribution of two peaks is not used because the distribution is assumed to be the Gaussian distribution. Meanwhile, the particles can approximate the state distribution accurately even when the state distribution has two peaks. As the information about the state and the measurement is increased with the passage of time, the sign of the state is cleared. Therefore, EKF can find the sign of the state. However, EKF, which cannot approximate the state distribution of two peaks, takes longer time than PF to find it. Consequently, the state estimation performance of PF is higher than that of EKF. In addition, PF can keep some possibilities of the state as the particles approximate the state distribution, which has two peaks, precisely. Therefore, PF can detect the step change of processes rapidly.

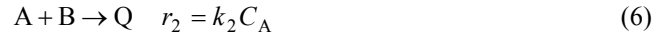
4. TUBULAR MICROREACTOR

Tubular microreactor (TMR) is a typical microreactor. TMR is used to produce radical polymer; the polymerization of butyl acrylate (Iwasaki and Yoshida, 2006), for example. To apply TMR to the real production, it is necessary to develop a system that can monitor the operation condition of TMR. However, the installation of sensors into the miniaturized space sometimes disturbs the flow. In addition, the existing miniaturized sensors are too expensive. Therefore, it is desirable to estimate the unmeasured states and unknown parameters of TMR from the limited number of the indirect measurements, which is not installed into the flow. In this work, one measurement, wall temperature, is used to estimate unknown parameters such as catalyst efficiency. Few researches on the estimation problems of TMR have been reported. In this section, the physical model and process model of TMR are explained. In addition, an estimation problem of TMR is solved with two kinds of filters, EKF and PF.

4.1 Process Model

Figure 3 shows a schematic diagram of TMR which is composed of inner channel, outer channel, inner wall and outer wall. Premixed reactants, A and B, are fed into the inner channel, and a coolant is fed into the outer channel.

Each flow is assumed to be plug flow (Peclet number = $100 > 1$), and the inner wall surface is coated with a catalyst. On the catalyst surface, the following sequential and parallel reactions take place.



P is the desired product, and Q and R are by-products. C is the concentration of each material. Reaction rate constant k_i ($i = 1, 2, 3$) is expressed by Arrhenius form.

$$k_i = A_i \exp(-E_i / RT_s) \quad (8)$$

Frequency factor A_i , activation energy E_i and constant heat of reaction ΔH_i in each reaction are shown in Table 2. T_s is the catalyst surface temperature. A and P are selected as key components, and heat and mass balances are described by the following equations:

$$\frac{\partial C_i}{\partial t} = -v \frac{\partial C_i}{\partial z} + D \frac{\partial^2 C_i}{\partial z^2} + D \frac{\partial^2 C_i}{\partial r^2} + D \left(\frac{1}{r} \right) \frac{\partial C_i}{\partial r} \quad (9)$$

$$\frac{\partial T_f}{\partial t} = -v \frac{\partial T_f}{\partial z} + \frac{k_f}{\rho_f C_{pf}} \frac{\partial^2 T_f}{\partial z^2} + \frac{k_f}{\rho_f C_{pf}} \frac{\partial^2 T_f}{\partial r^2} + \frac{k_f}{\rho_f C_{pf}} \left(\frac{1}{r} \right) \frac{\partial T_f}{\partial r} \quad (10)$$

$$\frac{\partial C_{As}}{\partial t} = -v \frac{\partial C_{As}}{\partial z} + D \frac{\partial^2 C_{As}}{\partial z^2} - \frac{k_C}{\delta} \left(C_{As} - C_A \Big|_{r=\frac{\delta}{2}} \right) - k_1 C_{As} - k_2 C_{As} \quad (11)$$

$$\frac{\partial C_{Ps}}{\partial t} = -v \frac{\partial C_{Ps}}{\partial z} + D \frac{\partial^2 C_{Ps}}{\partial z^2} - \frac{k_C}{\delta} \left(C_{Ps} - C_P \Big|_{r=\frac{\delta}{2}} \right) + k_1 C_{As} - k_3 C_{Ps} \quad (12)$$

$$\frac{\partial T_s}{\partial t} = -v \frac{\partial T_s}{\partial z} + \frac{k_f}{\rho_f C_{pf}} \frac{\partial^2 T_s}{\partial z^2} - \frac{U}{\delta} \left(T_s - T_f \Big|_{r=\frac{\delta}{2}} \right) - \frac{U}{\delta} \left(T_s - T_w \Big|_{r=\frac{\delta}{2}} \right) \quad (13)$$

$$- (\Delta H_1 k_1 C_{As} + \Delta H_2 k_2 C_{As} + \Delta H_3 k_3 C_{Ps}) / (\rho_f C_{pf}) \quad (14)$$

where z and r are the axial and radial coordinates, and other variables are explained in Table 3. As well, subscripts s, f and w present catalyst surface, fluid and wall, respectively. The catalyst thickness, δ , is 0.2 mm. In addition, the discrete approximation of Eqs. (9)-(14) using the orthogonal collocation method converted them into the state space model. The number of discrete points obtained from the roots of Chebyshev polynomial is 10 axially and 5 radially. In the following sections, Eqs. (9)-(14) are regarded as a real process, and the state space model as a process model.

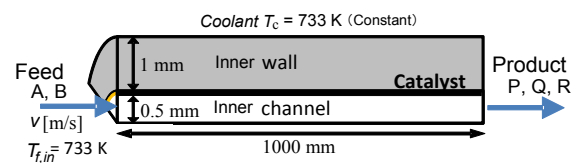


Fig. 3. Schematic diagram of MCF (Tonomura et. al., 2008).

Table 2. Reaction parameters.

Reaction	A_i [1/s]	E_i [J/mol]	ΔH_i [kJ/mol]
(1)	86760	71711.7	-2980
(2)	37260	71711.7	-4622
(3)	149.4	36026.3	-1664

Table 3. Model parameters.

Parameter	Value
reactant velocity v	1 m/s
mass diffusion coefficient D	1×10^{-5} m ² /s
heat diffusion coefficient k_f	0.041 J/m K s
heat conductivity of wall k_w	16.3 J/m K s
density of reactant ρ_f	1.01 kg/m ³
density of wall ρ_w	8000 kg/m ³
viscosity of fluid μ	2.92×10^{-5} Pa s
heat capacity of reactant C_{pf}	1090 J/kg K
heat capacity of wall C_{pw}	500 J/kg K
reactor length L	1 m
channel diameter d	1 mm
wall thickness d_w	1 mm
inlet concentration of species A C_A	4 mol/m ³
inlet concentration of species P C_P	0 mol/m ³
inlet temperature of reactant $T_{f,in}$	733 K
coolant temperature T_c	733 K

4.2 Sensor Location

The sensor location must be optimized so as to estimate unknown parameters most accurately. In this work, the optimal sensor location is determined based on the observability. When the dimension of the state vector is large, calculating the observability covariance W_o considering perturbation of all states takes the large computational load. Therefore, W_o is segmented to reduce the computational load:

$$W_o = \begin{bmatrix} W_o^{nn} & W_o^{pn} \\ W_o^{np} & W_o^{pp} \end{bmatrix} \quad (15)$$

where W_o^{pp} is the observability covariance matrix about the perturbation of unknown parameters. In the parameter estimation, not W_o but W_o^{pp} is used. In this study, an unknown parameter, catalyst efficiency, is estimated, and W_o^{pp} is scalar because of a single-parameter estimation. Large W_o^{pp} corresponds to an increase in the observability, namely high estimation performance. Average W_o^{pp} for the perturbation, 0.1, 0.2, 0.3 and 0.4, of catalyst efficiency is plotted as a function of axial sensor location candidates obtained from the roots of Chebyshev polynomial in Fig. 4. The largest W_o^{pp} can be found at 0.117 m from the inlet of TMR.

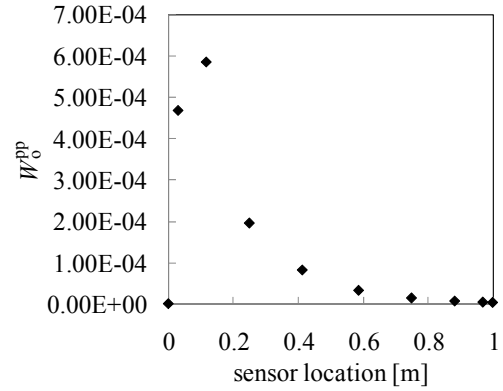


Fig. 4. W_o^{pp} at each sensor location.

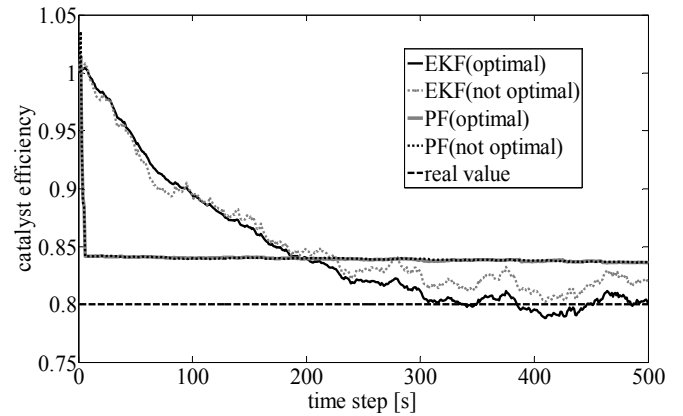


Fig. 5. Estimation results of EKF and PF.

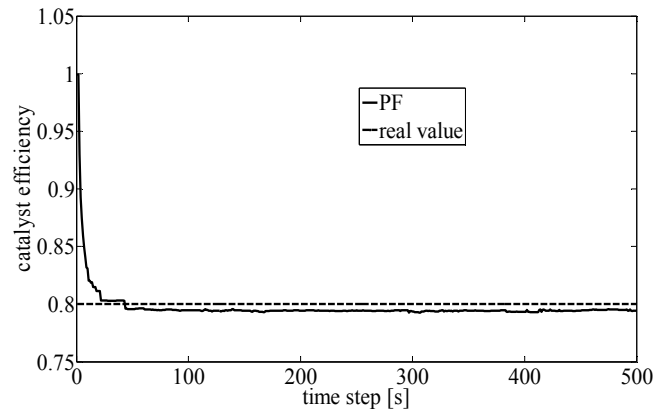


Fig. 6. Estimation result of PF.

4.3 Monitoring Results : Catalyst deterioration

The catalyst deterioration is detected through the parameter estimation of catalyst efficiency. The parameter estimation of catalyst efficiency is based on the process model of TMR. In this study, it is assumed that k_1 includes parameter α ($0 \leq \alpha \leq 1$) which indicates catalyst efficiency:

$$k_1 = \alpha A_1 \exp(-E_1 / RT_s) \quad (16)$$

α is assumed to be constant along TMR. TMR is in the steady state until $t = 0$. At $t = 0$, α is assumed to be changed

from 1 to 0.8. After catalyst deterioration, α is estimated from wall temperature by using EKF and PF. Sensor is located on the radial center of the wall. The number of particles in PF-based estimation is 100. Figure 5 shows the estimation results of α by EKF and PF. “optimal” and “not optimal” correspond to the sensor location, 0.117 m and 0.413 m from the inlet of TMR, respectively. The former sensor location was obtained in Section 4.2.

α can be estimated more rapidly and accurately by EKF (optimal) than EKF (not optimal). It is clarified that W_0^{PP} is effective for determining the optimal sensor location. In addition, PF can detect the change of α more rapidly than EKF. However, α cannot be estimated by PF accurately. This is due to the initial value of estimation. In PF, the estimation value is updated only through the system equation. Therefore, PF cannot estimate α accurately if the difference between the initial value and real value is large. Thus, to estimate α more accurately, larger system noise or the initial value with broader distribution, which has the possibility of α after step change, should be used. However, larger system noise causes violent oscillation of the estimation value. PF using the initial value of α with broader distribution is expected to follow α after step change rapidly. Figure 6 shows the estimation result of α by PF using the initial value of α set 0.6-1.0. Figure 7 shows the particle distribution of “PF (optimal) in Fig. 5”, PF (a), and “PF in Fig.6”, PF (b). Table 4 shows the simulation conditions of PF. In Fig. 5, PF (a) cannot estimate α accurately. Because the difference between the initial value of α and real value of α after step change is large as shown in Fig. 7. In Fig. 6, PF (b) can estimate α rapidly and accurately. This is because the initial distribution of α has the possibility of α after step change as shown in Fig. 7. Consequently, PF can detect the catalyst deterioration rapidly and accurately.

4.4 Monitoring Results : Blockage

The blockage is detected through the estimation of flow velocity. TMR is at steady state until $t = 0$ [s]. If the blockage happens under constant pumping pressure, the flow velocity decreases. In $t = 0-500$ [s], the flow velocity v is gradually changed from 1 to 0.8 [m/s]. v is estimated from one wall temperature using EnKF and PF. A temperature sensor is located at the radial center of the wall. The numbers of particles and ensemble members are both 100. Figure 8 shows the estimation results of PF and EnKF. Here “optimal” and “not optimal” correspond to the sensor location, 0.413 [m] and 0.0302 [m] from the inlet of TMR, respectively. PF (optimal) can estimate v more rapidly and accurately than PF (not optimal).

5. CONCLUSIONS

In this study, it was shown that the estimation performance of PF is better than that of EKF for nonlinear state space model of a lumped system through the numerical example. In addition, PF and EKF were applied to the change detection of the catalyst characteristics of TMR. It was found that PF can

Table 4. Simulation conditions of PF.

	Fig. 5 PF(optimal)	Fig. 5 PF (not optimal)	Fig. 6 PF
sensor location from the inlet [m]	0.117	0.413	0.117
initial value of α	same as EKF	same as EKF	0.6 ~ 1.0

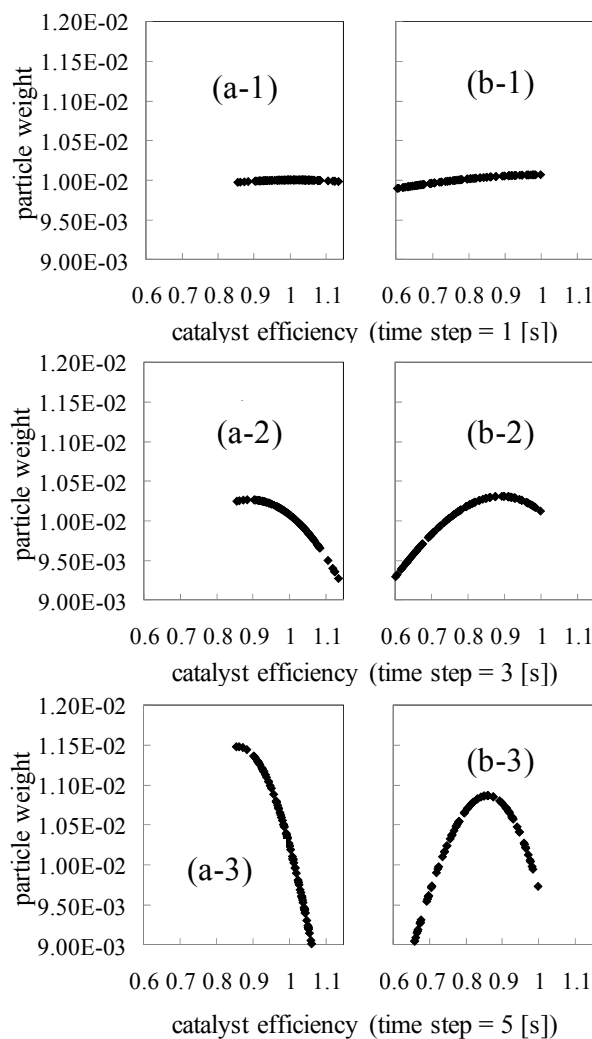


Fig. 7. Time transition of the particle distribution (a): PF (optimal) in Fig.5, (b): PF in Fig. 6.

detect the catalyst deterioration more rapidly and accurately than EKF. Moreover, PF and EnKF were applied to the change detection of the reactant flow velocity of TMR. It was shown that the blockage could be detected more rapidly and accurately by using PF than EnKF. PF is particularly promising for developing a process monitoring system for microreactors.

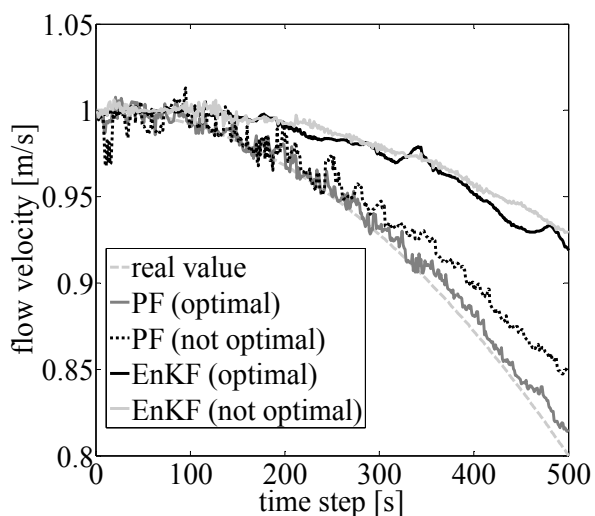


Fig. 8. Estimation results of EnKF and PF.

ACKNOWLEDGEMENT

This research was partially supported by the New Energy and Industrial Technology Development organization (NEDO), Project of Development of Microspace and Nanospace Reaction Environment Technology for Functional Materials.

REFERENCES

- Iwasaki, T. and Yoshida, J. (2005). Free radical polymerization in microreactors. significant improvement in molecular weight distribution control, *Macromolecules*, 38, 1159-1163.
- Kano, M., Fujioka, T., Tonomura, O., Hasebe, S., and Noda, M. (2007). Data-based and model-based blockage diagnosis for stacked microchemical processes, *Chem. Eng. Sci.*, 62, 1073-1080.
- Kitagawa, G. and Takemura, A. (2008). Statistical Sciences in the 21st Century, *University of Tokyo Press*, 305-338.
- Miyake, R. and Togashi, S. (2006). Innovation of chemical process engineering based on micro-reactor, *Professional Report*, 88(11), 916-917.
- Rawlings, J. B. and Bakshi, B. R. (2006). Particle filter and moving horizon estimation, *Compt. Chem. Eng.*, 30, 1529-1541.
- Tonomura, O., Kano, M., and Hasebe, S. (2008). Sensor location for effective fault diagnosis in micro chemical plants, *Proc. of Fifth International Conference on Foundations of Computer-Aided Process Operations (FOCAPO)*, 331-334.
- Yumimoto, K. (2009). Data assimilation methods with meteorological and chemical transport model, *Nagare*, 28, 37-44.